X-Ray Structures and Spectroscopic Studies of Diaqua- and Dichlorocopper(II) Complexes of 15-Crown-5 and 4′-Substituted Benzo-15-Crown-5 with a $3d_{z^2}$ Ground-State Doublet

Yong Li #

Graduate School of Human and Environmental Studies, Kyoto University, Kyoto 606

(Received April 18, 1996)

Crystallographic and spectroscopic investigations were carried out for Cu(II) complexes of 15-crown-5 (15C5) and 4′-substituted benzo-15-crown-5 (B15C5) derivatives. X-Ray diffraction measurements were performed for two single crystals of $[Cu(15C5)(H_2O)_2](ClO_4)_2$ and $[Cu(B15C5)(H_2O)_2](ClO_4)_2$, obtained from 60% $HClO_4$ solutions. The results of the X-ray analysis demonstrated that these complexes take a seven-coordinate pentagonal bipyramidal geometry, in which the copper ion is located in the center of the crown ether cavity with two water molecules at the axial positions. The ESR spectra observed for these complexes in 60% $HClO_4$ exhibited the characteristic g-anisotropy ($g_z < g_x, g_y$), leading to an electronic configuration of a $3d_{z^2}$ ground-state doublet. ESR and electronic absorption measurements were made for Cu(II) complexes of 4′-substituted B15C5 in systems of BF_3–ether–water and of dry $CHCl_3$ in which complexes having two chloride ions at the axial positions were produced. Although these systems showed the same remarkable substituent effects, clear differences were detected between them, attributable to the different axial ligands. The results of an extended Hückel MO calculation performed for the models of these complexes provide qualitative explanations for the experimental results.

It has been well known that most of Cu(II) complexes usually take four-coordinate square-planar or tetrahedral, and six-coordinate octahedral geometries. According to crystal field theory, the highest occupied level for a distorted tetrahedral and square-planar or elongated-octahedral geometries are deduced to be $3d_{xy}$ and $3d_{x^2-y^2}$, respectively. The electron configuration is referred to as a $3d_{xy}$ or $3d_{x^2-y^2}$ ground-state doublet, and their ESR spectra show the usual g-anisotropy as featured by $g_x, g_y < g_z$.[1] In addition, a six-coordinate Cu(II) complex with a compressed octahedral geometry is expected to take a $3d_{z^2}$ ground-state doublet, which reveals a typical g-anisotropy as $g_z < g_x, g_y$. However, Cu(II) complexes having a compressed octahedral geometry have been rarely reported.[2] Although a five-coordinate Cu(II) complex with a trigonal bipyramidal geometry has been predicted to take a $3d_{z^2}$ ground-state doublet, there are only limited examples.[3]

From the viewpoint of crystal field theory, a seven-coordinate Cu(II) complex with a pentagonal bipyramidal geometry has also been thought to take a $3d_{z^2}$ ground-state doublet. The seven-coordinate Cu(II) complexes have attracted the intense interest of many coordination chemists. However, little has been known about the electronic and coordination structures, since it is difficult to prepare Cu(II) complexes with a pentagonal bipyramidal structure. Until the work of Ishizu's group was reported,[4] no Cu(II) complex had been reported, except for a single crystal of a complex salt, $[K_3Cu(NO_2)_5]$, in which a part of the Cu(II) ions were located in a large distorted seven-coordinate environment, and its distorted, broad ESR lines provided little information.[5]

Ishizu and his co-workers[4] first indicated that 15-crown-5 (15C5) compounds are able to form pure $3d_{z^2}$ ground-state Cu(II) complexes in absolutely dry $CHCl_3$. A subsequent X-ray analysis of $[Cu(B15C5)Cl_2]$ complex (B15C5 stands for benzo-15-crown-5) revealed that the Cu(II) complex has a seven-coordinate pentagonal bipyramidal geometry, and two Cl^- counter anions axially coordinated to the Cu(II) ion.[6] On the other hand, similar $3d_{z^2}$-type Cu(II) complexes were also formed in BF_3–ether containing an optimum amount of water (hereafter BF_3–ether–water system). Based on the positive detection of ^{17}O ($I = 5/2$) superhyperfine splittings, derived from $H_2{}^{17}O$, in the g_z region of the ESR spectra, the presence of oxygenous ligands at axial positions have been confirmed. Although it is assumed in this case that the axial ligands are water molecules,[7] no direct X-ray proof was given in the previous work. So far, the studies on $3d_{z^2}$-type Cu(II) complexes of 15C5 compounds mainly focused on the axial ligands, and few detailed discussion were made concerning equatorial ligation. However, the author believes that a weak equatorial perturbation is important as well as a strong axial coordination for the formation of $3d_{z^2}$-type Cu(II) complexes. It is thus valuable to study the influences of not only the axial ligands, but also the equatorial ligation, on the coordination behavior with regard to $3d_{z^2}$-type Cu(II) complexes of 15C5 and related O_5-crown ethers.

In the present research, for the above purposes, Cu(II) complexes of 15C5 and 4′-substituted B15C5 were inves-

#The visiting researcher from Department of Chemistry, Tsinghua University, Beijing 100084, China.

tigated by means of X-ray diffraction, ESR and electronic spectroscopies. X-Ray structure analyses of single crystals obtained from $HClO_4$ solutions containing $Cu(ClO_4)_2$ and 15C5 or B15C5 provide direct evidence that two water molecules are axially coordinated to a Cu(II) ion in a seven-coordinate pentagonal bipyramidal geometry. The Cu–O distances in the apical positions are significantly shorter than those in the equatorial positions, as well as in the case of the $[Cu(B15C5)Cl_2]$ complex.[6] The ESR parameters of the Cu(II) complexes in $HClO_4$ exhibit a $3d_{z^2}$ ground-state doublet ($[Cu(15C5)(H_2O)_2]^{2+}$: $g_x=2.377$, $g_y=2.324$, $g_z=1.994$, and $[Cu(B15C5)(H_2O)_2]^{2+}$: $g_x=2.376$, $g_y=2.316$, $g_z=1.992$) which are consistent with those observed for BF_3–ether–water system. Further, ESR and electronic absorption measurements were performed for Cu(II) complexes of 4′-substituted B15C5, prepared not only in BF_3–ether–water, but also in dry $CHCl_3$ systems. Significant substituent effects on the spectroscopic parameters were recognized for these complexes. Extended Hückel molecular orbital (EHMO) calculations were also performed for models based on the X-ray structural data, and give satisfactory explanations for the observed results. The author wishes to report here on these results.

Experimental

Materials. Figure 1 shows the crown ethers used in the present work. 15C5 and 4′-substituted B15C5 were prepared and purified according to procedures given in the referenced papers.[8] The other chemical reagents, purchased from a Wako or a Nacalai Tesque Chemical Ltd., were guaranteed reagents, and were used without any further purification (excepting special notice[4]).

Single crystals were prepared as follows. A 2.0 mol dm^{-3} aqueous solution (0.16 ml) of $Cu(ClO_4)_2$ was added into a 0.06 mol dm^{-3} solution (5.0 ml) of 15C5 dissolved in 60% $HClO_4$. After standing for two or three days, colorless single crystals of diaqua(15C5)copper(II) perchlorate ($[Cu(15C5)(H_2O)_2](ClO_4)_2$, denoted as **A**) were obtained. Red single crystals of diaqua(B15C5)copper(II) perchlorate ($[Cu(B15C5)(H_2O)_2](ClO_4)_2$, denoted as **B**) were also obtained using the same method.

15C5 (or B15C5) and $Cu(ClO_4)_2\cdot 6H_2O$ in a molar ratio of 10:1 were dissolved in 60% $HClO_4$ for ESR measurements. The BF_3–ether–water solutions of Cu(II) complexes were prepared by mixing BF_3–ether solutions of 15C5 compounds and an aqueous solution of copper(II) salts.[9] Dry $CHCl_3$ solutions were produced by mixing anhydrous cupric chloride and the crown ethers with dry $CHCl_3$. The details concerning the preparations were described in previous papers.[4,7]

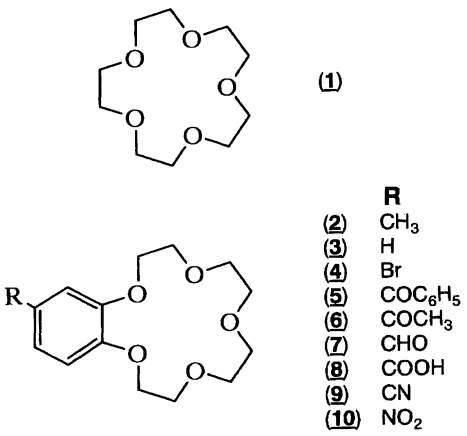

Fig. 1. Chemical structures of crown ethers.

X-Ray Crystal and Molecular Structure Analyses. A block crystal of **A** having approximate dimensions of $0.300\times0.300\times0.200$ mm was mounted on a glassfiber, and a block crystal of **B** having a size of $0.300\times0.300\times0.300$ mm was sealed in a glass capillary. All of the measurements were performed on a Rigaku AFC5R diffractometer with graphite-monochromated Mo $K\alpha$ radiation ($\lambda=0.71069$ Å) from a fine-focus anode of a 12 kW rotating-anode generator. The cell constants were estimated from a least-squares refinement using the respective 25 carefully centered reflections. The crystal data and details concerning the structure refinement are given in Table 1. Empirical absorption corrections based on azimuthal scans of several reflections[10] were applied, which resulted in transmission factors ranging from 0.80 to 1.00 for **A** and from 0.89 to 1.00 for **B**. The data were corrected for Lorentz and polarization effects. The corrections for secondary extinction were applied (coefficient $=1.1681\times10^{-6}$ for **A**, and 1.5749×10^{-6} for **B**).

The structures were solved by direct methods for **A** and a combination of the Patterson method and direct methods for **B**.[11] The coordinates and anisotropic temperature factors for the non-hydrogen atoms were refined by the full-matrix least-squares procedure based on F with weight $w=1/\sigma^2(F)$ for **A** and on F^2 with weight $w=1/\sigma^2(F^2)$ for **B**. The positions of the hydrogen atoms were idealized (C–H 0.95 Å), assigned isotropic thermal parameters $B(H)=1.2B_{eq}(C)$ and allowed to ride on their parent carbon atoms. All of the calculations were carried out on a VAX station 3200 computer with the TEXSAN program,[12] which used the atomic-scattering factors taken from the International Tables for X-Ray Crystallography.[13] Anomalous dispersion effects were included in the F_c calculation.

ESR and Electronic Absorption Measurements. The ESR measurements were carried out at 77 K using a JEOL-FE-2XG X-band spectrometer operating with a 100 KHz magnetic field modulation. The g-values were determined by taking Li-TCNQ ($g=2.0025$) as an external standard. The magnetic fields were calibrated based on the hyperfine splitting of Mn(II) doped in MgO (8.69 mT). The electronic absorption spectra were recorded with a Shimadzu UV-vis-NIR Scanning Spectrophotometer at room temperature.

EHMO Calculations. All of the molecular-orbital calculations were performed using the extended Hückel method. EHMO calculations were performed with a program developed by Nishimoto et al.[14] In order to obtain simplified results, $[Cu(H_2O)_7]^{2+}$ (**I**) and $[Cu(H_2O)_5Cl_2]$ (**II**) with D_{5h} symmetry were used as models of $[Cu(15C5)(H_2O)_2]^{2+}$ and $[Cu(15C5)Cl_2]$. In addition, simple models of $[Cu(B15C5)(H_2O)_2]^{2+}$ and its derivatives, and of $[Cu(B15C5)Cl_2]$ used for the calculation, are shown in Fig. 2.[15] The Cu(II) ion is placed at the origin. All of the equatorial ligands are located in the xy plane, and the axial ones are taken along the z-axis. The distances between the Cu(II) ion and the coordinated atoms in the equatorial and axial positions are taken to be the average values obtained from the present and previous X-ray analyses,[6] respectively. The standard values were used for the other bond lengths and angles.[16] The atomic parameters used in the EHMO calculations for H, C, N, O, and Cl are the standard ones.[17] The atomic energies (H_{ii}) of Cu(II) were obtained from self-consistent charge (scc) calculations.[17] The 4s and 4p exponents for Cu(II) were taken from Hoffmann et al.,[18] and the two-component 3d orbital of Cu(II) is from Richardson et

Table 1. Crystal Data, Structure Determination and Refinement Data for **A** and **B**

	A	**B**
Formula	$C_{10}H_{24}O_{15}Cl_2Cu$	$C_{14}H_{24}O_{15}Cl_2Cu$
M.W.	518.74	566.79
Crystal system	Monoclinic	Monoclinic
a/Å	14.121(2)	9.690(2)
b/Å	16.834(2)	16.521(3)
c/Å	8.698(1)	14.373(1)
β/°	100.38(1)	102.08(1)
V/Å^3	2033.9(9)	2250.0(6)
Space group	$C2/c$	$P2_1/n$
Z	4	4
D_c/g cm^{-3}	1.694	1.673
μ/cm^{-1}	13.95	12.80
Radiation (λ/Å)	Mo $K\alpha$ (0.71069)	Mo $K\alpha$ (0.71069)
Scan method	ω–2θ	ω–2θ
2θ range/°	6.0—55.0	6.0—55.0
Scan speed/° min^{-1}	16.0	16.0
Scan width/°	1.63+0.30tan θ	0.94+0.30tan θ
Standard reflcns	Three every 100 reflcns	Three every 100 reflcns
No. of data measd	2519	5676
No. of unique data (R_{int})	2424(0.025)	5369(0.042)
No. of obsd data	1693($I > 3.0\sigma(I)$)	2412($I > 1.5\sigma(I)$)
No. of variables	145	342
R; R_w	5.8; 7.6	7.3; 6.9
S, goodness of fit	2.20	1.82
Range of (Δ/ρ)/e$^-$Å^{-3}	−0.61 to 0.92	−0.44 to 0.60

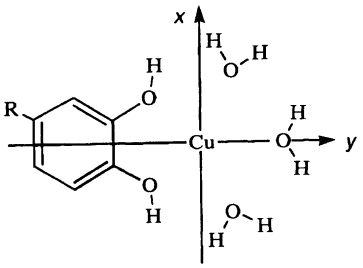

	R	Axial Ligand
(III)	H	H_2O
(IV)	CH_3	H_2O
(V)	NO_2	H_2O
(VI)	H	Cl

Fig. 2. Models for Cu(II) complexes of 4′-substituted B15C5 used for EHMO calculations.

al.[19] Table 2 summarizes the extended Hückel parameters used for the Cu(II) complexes. A "weighted H_{ij}", which is the modified Wolfsberg–Helmholz formula, was used in all of the calculations according to Hoffmann et al.'s method.[20]

Results

Molecular Structures of $[Cu(15C5)(H_2O)_2]^{2+}$ and $[Cu(B15C5)(H_2O)_2]^{2+}$. PLUTO drawings of the molecular structures for cations of **A** and **B** are shown in Fig. 3,[21] together with the atomic-numbering scheme. The final atomic parameters and equivalent isotropic thermal parameters are given in Tables 3 and 4. Table 5 gives the pertinent bond lengths and bond angles for both Cu(II) complexes. The final atomic parameters involving the hydrogen atoms, together with the observed and calculated structure factors, have been deposited as Document No. 69047 at the Office of the Editor of Bull. Chem. Soc. Jpn.

As shown in Fig. 3, X-ray structural analyses of **A** and **B** revealed that the coordination geometries take a seven-coordinate pentagonal bipyramid with an approximate D_{5h} symmetry (Table 5). The five ethereal oxygen atoms are nearly planar. In the case of **A**, there exists a C_2 axis through Cu and O(3). O(2) and O(2*) deviate by ±0.485 Å from

Table 2. Parameters for Cu(II) Ion Used in the EHMO Calculations of Model Complexes

	Orbital exponent		H_{ii}[a]					
Orbital	1	2	**I**	**II**	**III**	**IV**	**V**	**VI**
3d	5.95(0.6062)[b]	2.50(0.5731)[b]	14.62	14.61	13.017[c]	12.915[c]	13.120[c]	12.834[c]
4s	2.200		12.50	12.49	10.80	10.69	10.92	10.59
4p	2.200		7.66	7.65	6.33	6.24	6.42	6.17

a) H_{ii} in eV. b) Numbers in parentheses indicate the coefficient of the member of the contracted 3d function. c) H_{ii} values of 3d orbital must be more carefully controlled for scc calculations.

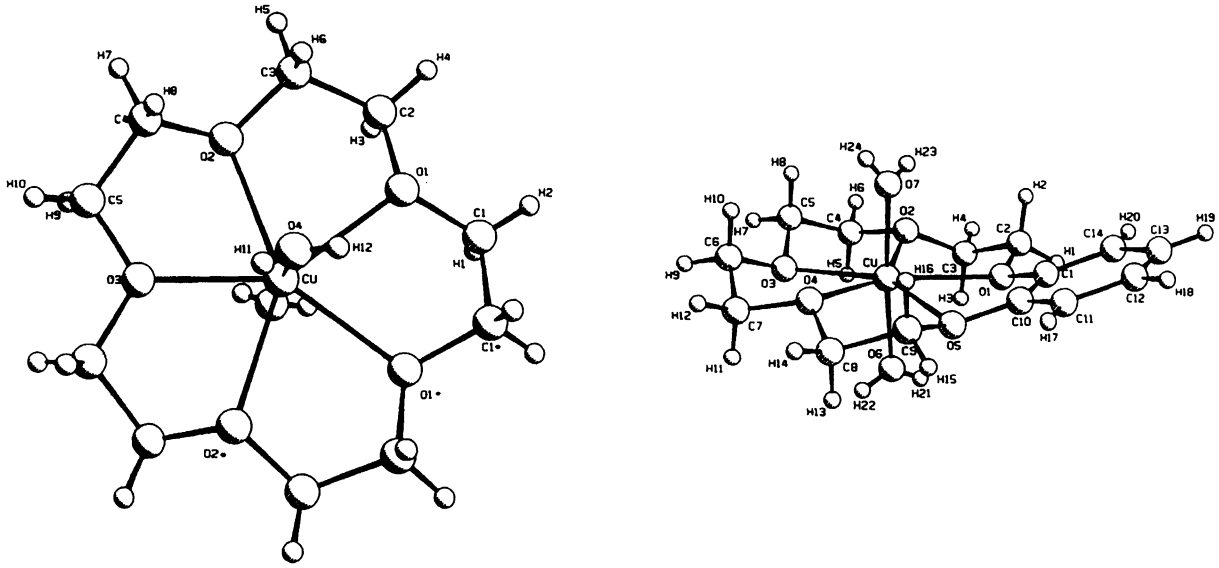

Fig. 3. PLUTO drawings of $[Cu(15C5)(H_2O)_2]^{2+}$ (left) and $[Cu(B15C5)(H_2O)_2]^{2+}$ (right), together with the atomic-numbering schemes.

Table 3. Fractional Positional Parameters and Thermal Parameters of Non-Hydrogen Atoms with Their esd in Parentheses for **A**

Atom	x	y	z	B_{eq}/Å^2
Cu	0.0000	0.23623(5)	0.2500	2.96(4)
Cl	0.2417(1)	0.40250(9)	0.0142(2)	4.27(6)
O(1)	−0.0472(3)	0.1303(2)	0.1032(5)	5.0(2)
O(2)	−0.1062(3)	0.2806(3)	0.0330(5)	5.8(2)
O(3)	0.0000	0.3630(3)	0.2500	4.8(3)
O(4)	0.1077(5)	0.2355(3)	0.1449(9)	6.2(3)
O(5)[a)]	0.2182(6)	0.3648(5)	0.1462(9)	12.6(5)[b)]
O(6)	0.1889(8)	0.3600(7)	−0.102(1)	17.1(7)
O(7)	0.2292(6)	0.4798(4)	0.027(1)	18.4(8)
O(8)	0.3414(5)	0.3856(5)	0.030(1)	12.0(5)
C(1)	−0.0461(5)	0.0588(4)	0.1918(9)	5.4(3)
C(2)	−0.1320(6)	0.1432(5)	−0.009(1)	7.2(4)
C(3)	−0.1210(7)	0.2221(5)	−0.0848(9)	7.6(4)
C(4)	−0.0755(6)	0.3550(4)	−0.0142(8)	6.0(3)
C(5)	−0.0532(5)	0.4069(4)	0.1267(8)	5.5(3)

a) Oxygen atoms with numbers from (5) to (8) are ones of the perchlorate ion. b) The large temperature factors of the oxygen atoms in the perchlorate ion can be attributed to high thermal motion or disordering, but the conventional X-ray structure analysis can not discriminate them.

the plane of O(3), O(1), and O(1*); thus, the Cu(II) ion lies just in the same plane. On the contrary, in the case of **B**, O(2) and O(4) deviate by 0.314 and 0.366 Å, respectively, toward O(7) from the plane defined by the other ethereal oxygen atoms; the Cu(II) ion is situated in this plane with a deviation of 0.151 Å. For both complexes, the 15-membered ring has a crown-type conformation. All of the frameworks of C–O–C–C take a nearly *anti*-conformation, and those of O–C–C–O take a nearly *gauche* conformation, except for that of O(1)–C(1)–C(10)–O(5) in **B**, which is frozen by the benzene ring. The equatorial Cu–O distances are 2.133(5)—2.313(4) Å for **A** and 2.150(6)—2.314(5) Å for **B**. Since they are approximately equal to the sum of the Cu(II) ion radius (0.87 Å)[22] and the van der Waals radius of the oxygen atom (1.40 Å),[16] the equatorial bonding nature may be primarily due to the ion-dipole static-electronic interaction.

X-Ray structure analyses demonstrated that for each complex two water molecules axially coordinate to the Cu(II) ion above and below the positions of the crown ring. The apical Cu–O distances (1.910(5) Å for **A**, 1.922(6) and 1.913(5) Å for **B**) are significantly shorter than the equatorial Cu–O distances. Furthermore, they are also shorter than most of the equatorial Cu–O distances (1.92—2.15 Å), which are generally shorter than the apical ones in octahedral Cu(II) complexes.[23] Because the minimal Cu–O distance has been estimated to be about 1.92 Å for the chromophore CuO_6,[23] one can be convinced that in the present complexes the axial coordination bonds are considerably strong and mainly covalent. This fact is consistent with the previous proposal derived from ESR studies that the electronic configuration of a $3d_{z^2}$ ground-state is caused by strong axial ligation.

In a comparison of the molecular structure of **B** with that

Table 4. Fractional Positional Parameters and Thermal Parameters of Non-Hydrogen Atoms with Their esd in Parentheses for **B**

Atom	x	y	z	$B_{eq}/Å^2$
Cu	0.48595(9)	0.11837(5)	0.21247(6)	4.15(3)
Cl(1)	0.6556(3)	−0.1712(1)	0.3078(2)	7.7(1)
Cl(2)	0.0844(2)	−0.1037(1)	0.1276(2)	6.0(1)
O(1)	0.6939(5)	0.0677(3)	0.2916(4)	5.2(2)
O(2)	0.6374(6)	0.1234(3)	0.1192(4)	6.8(3)
O(3)	0.3586(7)	0.1492(3)	0.0690(5)	9.1(4)
O(4)	0.2844(6)	0.1550(3)	0.2384(5)	7.3(3)
O(5)	0.4801(5)	0.0845(3)	0.3678(3)	5.2(2)
O(6)	0.4396(7)	0.0073(3)	0.1807(5)	5.8(3)
O(7)	0.5408(7)	0.2267(3)	0.2505(5)	6.7(3)
O(8)[a]	0.564(1)	−0.1127(5)	0.3017(7)	17.2(6)[b]
O(9)	0.636(1)	−0.2223(6)	0.3802(8)	18.6(8)
O(10)	0.773(1)	−0.1408(8)	0.329(2)	33(2)
O(11)	0.670(1)	−0.2193(6)	0.2378(7)	18.4(8)
O(12)[c]	0.184(1)	−0.0542(9)	0.100(1)	8.9(7)
O(12P)	0.157(2)	−0.0392(8)	0.166(1)	10.0(8)
O(13)	0.066(2)	−0.116(1)	0.0325(8)	14(1)
O(13P)	0.113(3)	−0.168(1)	0.110(3)	31(2)
O(14)	0.164(4)	−0.155(2)	0.184(2)	28(2)
O(14P)	0.102(3)	−0.170(1)	0.172(2)	22(2)
O(15)	−0.063(2)	−0.091(1)	0.101(2)	18(1)
O(15P)	0.012(2)	−0.070(1)	0.188(1)	16(1)
C(1)	0.7230(9)	0.0763(4)	0.3896(6)	5.8(4)
C(2)	0.8079(9)	0.0713(5)	0.2432(8)	8.0(5)
C(3)	0.744(1)	0.0628(6)	0.1401(8)	8.8(5)
C(4)	0.571(2)	0.1282(6)	0.0232(8)	11.3(7)
C(5)	0.451(2)	0.1826(6)	0.0110(7)	11.7(7)
C(6)	0.244(1)	0.1995(6)	0.078(1)	11.7(7)
C(7)	0.175(1)	0.1629(6)	0.149(1)	11.3(7)
C(8)	0.240(1)	0.1188(6)	0.314(1)	10.6(6)
C(9)	0.359(1)	0.1218(5)	0.3978(7)	7.9(4)
C(10)	0.604(1)	0.0850(4)	0.4300(6)	6.0(4)
C(11)	0.623(1)	0.0921(5)	0.5276(7)	8.9(6)
C(12)	0.759(2)	0.0891(6)	0.580(1)	13.6(8)
C(13)	0.874(1)	0.0826(7)	0.548(1)	12.7(7)
C(14)	0.859(1)	0.0752(5)	0.4455(8)	9.0(5)

a) Oxygen atoms with numbers from (8) to (11) are connected to Cl(1). b) See note b) in Table 3. c) Oxygen atoms from (12) to (15) connected to Cl(2) are divided into two sets labeled with and without P because of disordering.

Table 5. Selected Bond Distances and Angles with Their esd in Parentheses for **A** and **B**

Bond distances/Å		Bond angles/°	
A			
Cu–O(1)	2.225(4)	O(1)–Cu–O(2)	73.0(2)
Cu–O(2)	2.313(4)	O(2)–Cu–O(3)	71.2(1)
Cu–O(3)	2.133(5)	O(1)–Cu–O(1*)	73.4(2)
Cu–O(4)	1.910(5)	O(4)–Cu–O(3)	90.4(2)
B			
Cu–O(1)	2.257(5)	O(1)–Cu–O(2)	71.3(2)
Cu–O(2)	2.186(5)	O(2)–Cu–O(3)	74.7(3)
Cu–O(3)	2.229(6)	O(3)–Cu–O(4)	75.5(3)
Cu–O(4)	2.150(6)	O(4)–Cu–O(5)	72.2(2)
Cu–O(5)	2.314(5)	O(5)–Cu–O(1)	67.9(2)
Cu–O(6)	1.922(6)	O(6)–Cu–O(3)	86.7(2)
Cu–O(7)	1.913(5)	O(7)–Cu–O(6)	176.5(3)

of [Cu(B15C5)Cl_2] (**C**) obtained in dry $CHCl_3$,[6] one can find that all of the equatorial Cu–O distances in **B** are shorter than the corresponding bond lengths of **C** in magnitude of 0.02—0.10 Å; also, the apical Cu–O bond lengths of **B** are markedly shorter than the axial Cu–Cl ones (2.254(2) and 2.242(2) Å) in **C**. These results show that the dihydrated complex (**B**) has a more compact coordination geometry than does the dichlorinated one (**C**), and that there is, accordingly, a correlation between the bonding nature of the apical bonds and that of the equatorial bonds. This leads to an idea to investigate the substituent effects on the spectroscopic properties of the complexes through the benzene ring of B15C5.

ESR Spectra. Some typical ESR spectra observed for the Cu(II) complexes in the BF_3–ether–water system and in dry $CHCl_3$ are shown in Fig. 4, together with those of [Cu(15C5)$(H_2O)_2$]$(ClO_4)_2$ and [Cu(B15C5)$(H_2O)_2$]$(ClO_4)_2$ in 60% $HClO_4$. The ESR parameters obtained for all of those are summarized in Table 6, in which the apparent g_x and g_y values correspond to the positions indicated by the arrow marks in Fig. 4. Based on the ESR spectra, and taking account of the g parameters ($g_z < g_x, g_y$), one can see that all of the present Cu(II) complexes possess a $3d_{z^2}$ ground-state, which indicates that the Cu(II) ion is captured in the cavity of the crown ether ring.

Obviously, the Cu(II) complexes in the BF_3–ether–water system and in 60% $HClO_4$ have similar ESR parameters and line shapes. It is thus believed that the Cu(II) complexes in the system containing water have the same coordination environment. However, a large excess of the crown ethers is necessary to obtain the ESR spectra only contributed from the $3d_{z^2}$ ground-state Cu(II) complexes in 60% $HClO_4$, because equilibrium takes place between the Cu(II) complexes and $[Cu(H_2O)_6]^{2+}$ in the presence of a large amount of water in solution. If the ligand compounds are not sufficient, one observes an overlap of the ESR signals due to two types of Cu(II) complexes with $3d_{z^2}$ and $3d_{x^2-y^2}$ ground-states. In addition, because of strong oxidation by $HClO_4$, not only an unwanted ESR peak is frequently observed for solutions containing B15C5 or its derivatives, but also the color of the solutions changes. These phenomena concerning the Cu(II) complexes in 60% $HClO_4$ are disadvantageous for the ESR, and especially for visible electronic absorption measurements. Thus, BF_3–ether–water solutions were used instead of 60% $HClO_4$ solutions for all of the ESR and electronic absorption experiments.

The linewidth in the parallel components of the ESR spectra in dry $CHCl_3$ are much broader than those in the BF_3–ether–water system. This is because of an overlap of the ligand superhyperfine splittings due to two axially ligating chloride anions for the complexes in dry $CHCl_3$. The superhyperfine coupling constants (A_z^{Cl}) are also listed in Table 6. On the contrary, no important change and no superhyperfine structure in the ESR spectra was detected in a BF_3–ether–water system, although several cupric salts with

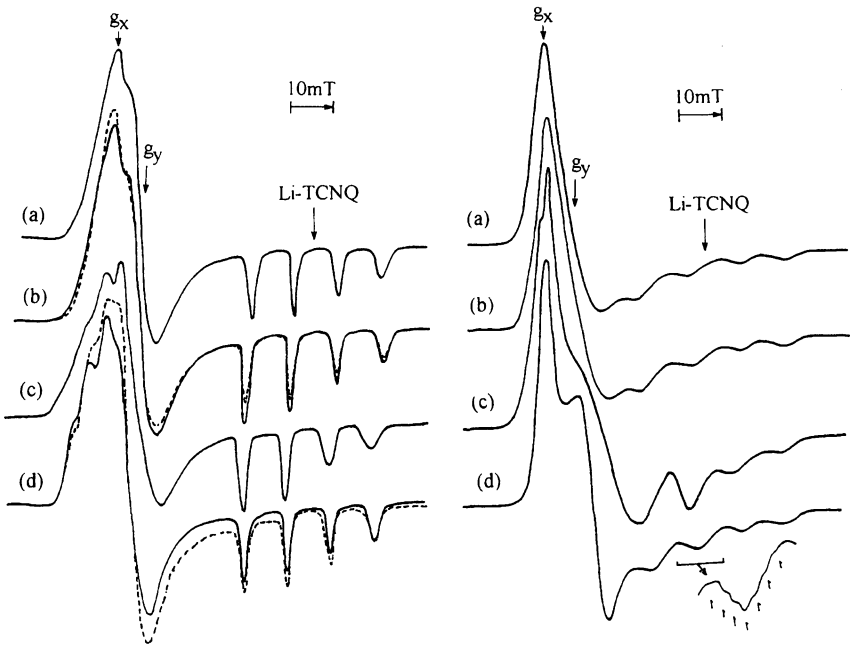

Fig. 4. ESR spectra observed at 77 K for the Cu(II) complexes of **2** (a), **3** (b), **10** (c), and **1** (d) in the BF_3–ether–water system (left) and in dry $CHCl_3$ (right). The broken lines represent the ESR spectra for the complexes in 60% $HClO_4$.

Table 6. ESR Parameters of the Cu(II) Complexes

Ligand	BF_3–ether–water system				Dry $CHCl_3$				
	g_x	g_y	g_z	$A_z^{a)}$	g_x	g_y	g_z	A_z	A_z^{Cl}
1	2.376	2.323	1.995	102.5	2.376	2.259	2.001	122.0	16.9
	(2.377)[b)]	(2.324)	(1.994)	(104.1)					
2	2.375	2.314	1.991	109.1	2.351	2.271	1.998	133.2	16.1
3	2.379	2.314	1.992	107.8	2.346	2.269	1.997	130.0	16.3
	(2.376)	(2.316)	(1.992)	(110.5)					
4	2.377	2.313	1.993	107.3	2.353	2.259	2.002	127.1	16.5
5	2.383	2.307	1.994	107.0	2.349	2.269	2.000	129.1	16.1
6	2.378	2.299	1.994	106.8	2.351	2.260	2.001	127.0	16.3
7	2.384	2.299	1.995	106.4	2.352	2.255	2.003	127.4	16.4
8	2.381	2.303	1.994	107.2		—	—	—[c)]	
9		—	—[d)]		2.356	2.254	2.000	124.9	16.9
10	2.378	2.298	1.995	102.5	2.354	2.227	2.008	121.7	16.7

a) A values in 10^{-4} cm^{-1}. b) The values in parentheses for the Cu(II) complexes in 60% $HClO_4$. c) Insoluble. d) Only showed a broad signal without hyperfine structure.

different anions, such as ClO_4^-, BF_4^-, SO_4^-, and F^-, were used. In the previous ESR study, we assumed that the Cu(II) ion in 15C5 or B15C5 complex is coordinated to water molecules at the apical positions in a BF_3–ether–water system, based on a positive detection of a superhyperfine splitting due to the ^{17}O isotope by using $H_2{}^{17}O$.[7] Thus, the same coordination environment has been confirmed for the present 4′-substituted B15C5 Cu(II) complexes. That is, the axial ligands are water molecules. This idea is also supported by the above-mentioned X-ray structure analyses. The ESR spectra of the 4′-substituted B15C5 Cu(II) complexes in either system show great changes in the perpendicular components. This implies a substituent effect on the ESR spectra.

The relationships between the g_z or g_y and A_z values of the Cu(II) complexes of 4′-substituted B15C5 are illustrated in Fig. 5. One can see that the values are located in two different areas for the complexes in the BF_3–ether–water system and in dry $CHCl_3$; especially a significant difference can be found in the A_z values. This reflects the difference in the coordination environments in the two systems, which is conceivable to be mainly due to the different axial ligands. In addition, it is worth noticing that in each system the complex with an electron-releasing group, such as methyl, has larger A_z and g_y values and a smaller g_z value, while the Cu(II) complex with an electron-withdrawing group, such as nitro, shows a reverse situation.

Electronic Spectra. In general, most Cu(II) complexes have a color of blue or green. It is of interest that the $[Cu(15C5)(H_2O)_2]^{2+}$ complex in the BF_3–ether–water system is colorless, and that the other complexes in both the systems

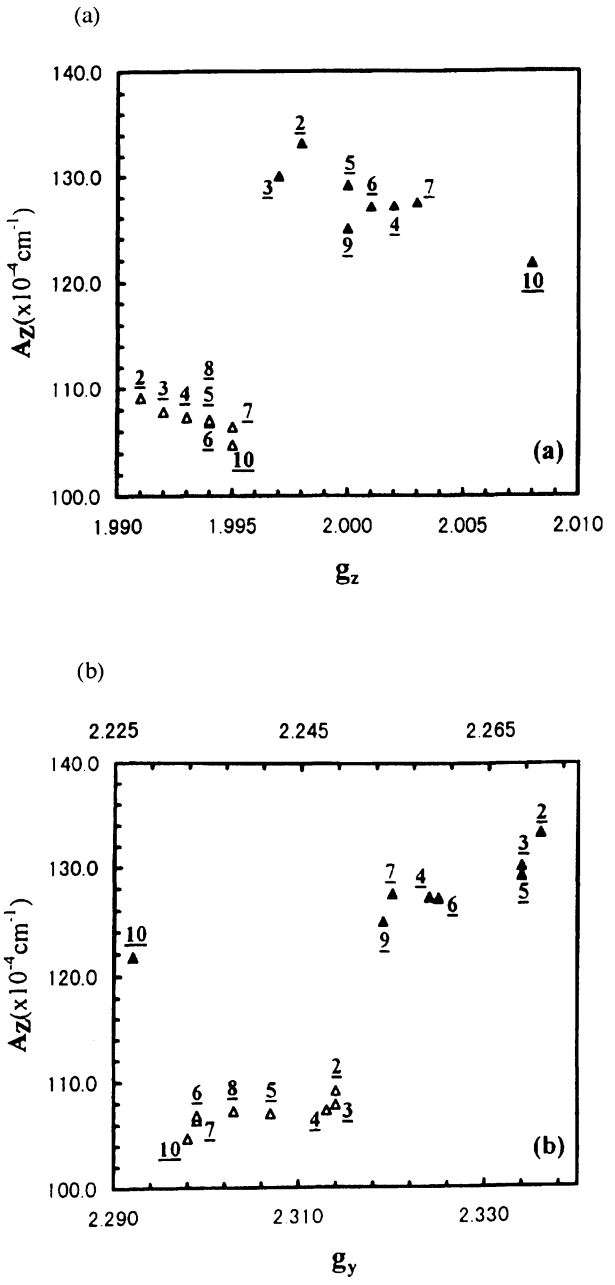

Fig. 5. Correlation diagrams between A_z and g_z (a) and g_y (b). Open and solid triangles, which follow the lower and upper horizontal axes in (b), represent the values obtained in the BF_3–ether–water system and in dry $CHCl_3$, respectively.

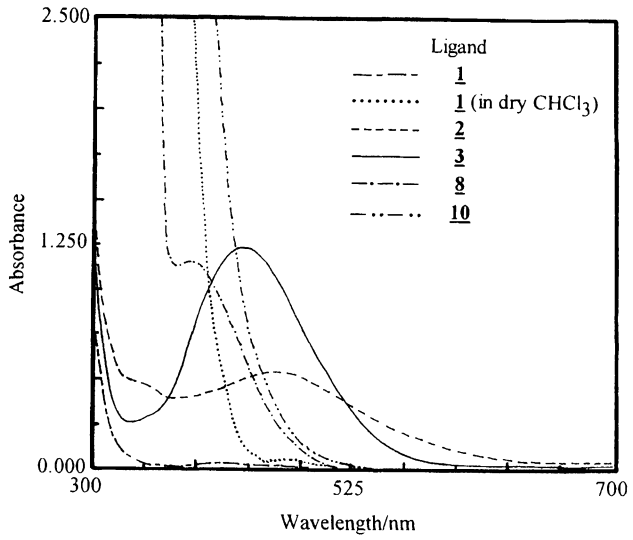

Fig. 6. Visible absorption spectra observed at room temperature for the Cu(II) complexes in the BF_3–ether–water system. Where the concentration of **2**–Cu(II) complex is a half of those for other complexes.

are red or yellow. Figure 6 shows their typical electronic absorption spectra. Clearly, no important absorption band in the visible region is detected for the $[Cu(15C5)(H_2O)_2]^{2+}$ complex, whereas a tail of the peak, which may originate from a charge transfer between the chloride anion and the central metal ion, can be found as far as about 440 nm for the $[Cu(15C5)Cl_2]$ complex having orange-yellow color in dry $CHCl_3$. On the other hand, the Cu(B15C5) complexes in both the systems give absorption peaks at about 430—440 nm, which has been attributed to a change transfer between the benzene molecular orbital and the copper 3d atomic orbital in a previous study.[7b] A substituent effect was clearly observed in the present work, as shown in Fig. 6 and Table 7. The electron-releasing group give a red shift and the electron-withdrawing group a blue shift. These findings also strongly hint that the bands are closely associated with the benzene molecular orbital. It will be interpreted by means of EHMO calculations later.

Although the d–d absorption bands of nearly all Cu(II) complexes are usually observed in the visible region, in the present research no corresponding d–d band was detected in the same region for all of the Cu(II) complexes in both the systems. They show broad, weak bands in the near-infrared region from 850 to 1600 nm, as shown in the previous paper, which were assigned to the copper d_{z^2}–d_{xz} and d_{z^2}–d_{yz} transitions based on the ESR parameters.[7b] It is interesting that the compared to the charge-transfer bands, the d–d bands are almost untouched by substituents. This means that the energy gap between d_{z^2} and d_{xz} or d_{yz} orbitals, which are out of the *xy* plane, is little affected by the substituents.

EHMO Calculations. The EHMO method, developed principally by Hoffmann,[24] has been widely and usefully applied to various organic compounds and metal complexes.[14] The present EHMO calculations were performed for models **I**, **II**, and the others shown in Fig. 2. For simplicity, Fig. 7 illustrates only the energy levels of MO's related to the valence orbitals of the Cu(II) ion calculated for **I** together with those necessary for the following discussions. Similar orders are also given for the remaining **II** to **VI**. The calculation revealed that HOMO (also referred as SOMO) in each model is an antibonding MO ($a_1'(\sigma^*)$), in which the main component is a $3d_{z^2}$ orbital. This is in excellent agreement with the fact obtained from ESR observations that the present Cu(II) complexes have a $3d_{z^2}$ ground-state. Obviously, from Fig. 7, the d levels are $d_{z^2}(a_1'(\sigma^*)) > d_{x^2-y^2}, d_{xy}(e_2'(\sigma^*)) > d_{xz}, d_{yz}(e_1''(\pi^*))$. This order is consistent with that in a pentagonal bipyrami-

Table 7. Visible Absorption Spectra Data of the Cu(II) Complexes of 4′-substituted B15C5

Ligand	BF_3–ether–water system		Dry $CHCl_3$	
	λ_{max} [a)]	ε [a)]	λ_{max}	ε
2	455	211	461	225
3	430	202	440	240
4	426	197	437	255
5	< 450	—	420	340
6	< 420	—	< 420	—
7	< 420	—	420	390
8	383	193	—	—
9	—	—	< 420	—
10	< 420	—	< 420	—

a) λ_{max} in nm and ε in $mol^{-1}\,dm^3\,cm^{-1}$.

dal field expected in terms of crystal field theory.[25]

The electron population at the Cu(II) ion calculated for **IV** increases compared with that of **III**, whereas that decreases for **V**. This is in good accordance with the observed change in the A_z values due to a substituent effect. Moreover, the calculation revealed that the lower symmetry of charge distribution in the equatorial positions is produced by the stronger electron-withdrawing group, because the charge on the oxygen atoms connected to the benzene ring (catechol oxygen atoms) is influenced by substituents, while the others almost do not. This fact provides a satisfactory explanation for the changes in the ESR spectra, as shown in Fig. 4.

The $[Cu(15C5)(H_2O)_2]^{2+}$ complex in the BF_3–ether–water system is colorless, while $[Cu(15C5)Cl_2]$ in dry $CHCl_3$ is orange-yellow (Fig. 6). This is understandable as follows in terms of the charge-transfer transition from axial ligands to the central copper(II) ion. In the present EHMO calculations, the energy differences between HOMO and LUMO (both centered on the 4s and $3d_{z^2}$ orbitals of the central metal) for **I** and **II** is too large to exhibit the HOMO→LUMO absorption band in the visible and near ultraviolet regions (Fig. 7). The energy level of the MO, centered mainly on the p_x and p_y orbitals of the axially coordinated atoms (dotted line in Fig. 7), follows d_{xz}, $d_{yz}(e_1''\ (\pi^*))$. The energy difference between this MO and HOMO is evidently decreased in **II** ($\Delta E = 1.292$ eV) by in contrast with that in **I** ($\Delta E = 1.432$ eV). The cor-

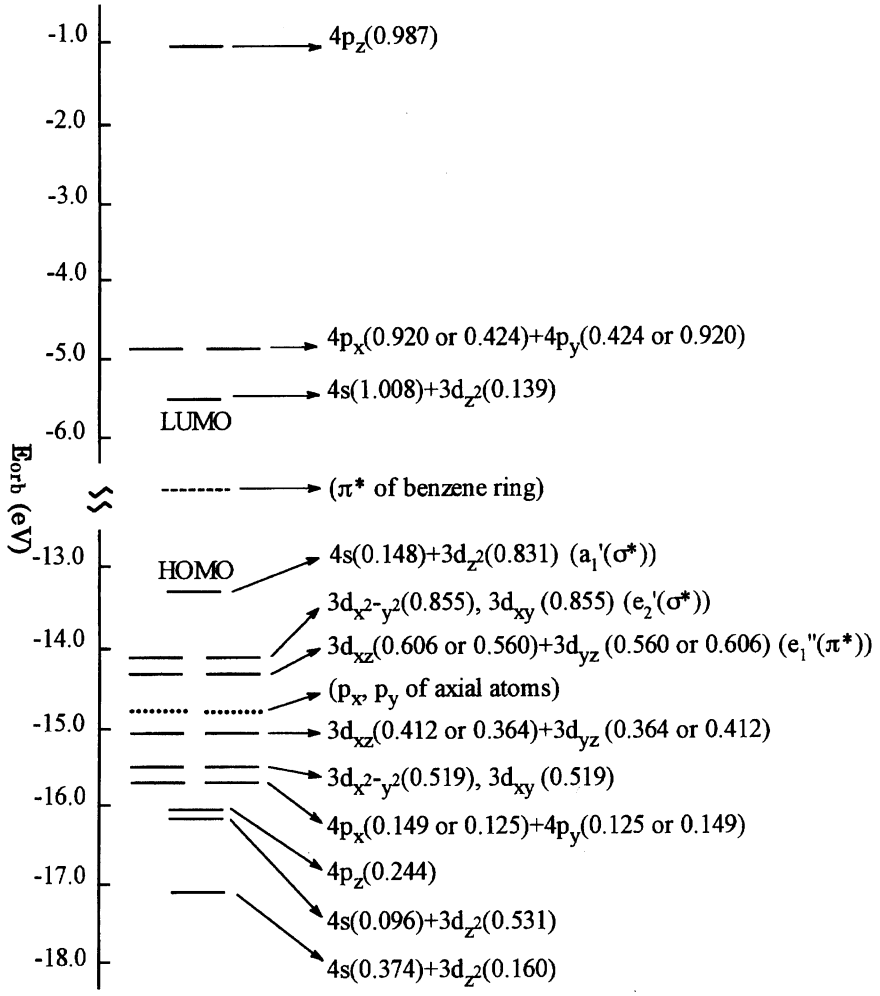

Fig. 7. Energy levels of MO's related to the valence orbitals of Cu(II) ion calculated for **I**. The values in parentheses indicate the MO coefficients of the atomic orbitals. Dotted lines represent the levels concerning p_x and p_y orbitals of axial ligands in **I** and **II**, and broken ones do π^* orbitals in the models containing benzene ring.

responding charge-transfer transition can explain the above color change of the complexes.

On the other hand, different from the instances of **I** and **II**, LUMO is a pure π^* orbital of the benzene ring for models **III**, **IV**, **V** and **VI** (broken line in Fig. 7). In these cases, taking account of the energy difference with HOMO and the substituent effect, it is guessed that a transition from HOMO to LUMO corresponds to the above-mentioned charge-transfer band for 4′-substituted B15C5 Cu(II) complexes. The energy difference between HOMO and LUMO (ΔE_{HL}) is reduced by the electron-releasing group, $-CH_3$ ($\Delta E_{HL,III} - \Delta E_{HL,IV} = 0.085$ eV, corresponding to red shift), whereas it is increased by the electron-withdrawing group, $-NO_2$ ($\Delta E_{HL,III} - \Delta E_{HL,V} = -0.121$ eV, corresponding to blue shift). This tendency agrees with the experimental substituent effect.

In the electronic absorption spectra, the charge-transfer peak is shifted toward long wavelengths in dry $CHCl_3$ compared with in the BF_3–ether–water system (see Table 7). Although an attempt was made to explain this red shift by EHMO calculations, it was found that the energy gap between HOMO and LUMO is almost unchanged for models **III** and **VI** shown in Fig. 2. Thus, the red shift may in principle be attributed to solvent effect, rather than the different axial ligands, since the position of a charge-transfer band is usually easily affected by solvents.

Usually, a transition-metal atom takes a d^3sp^3 hybrid in a D_{5h} field to form σ bonds, and d_{xz} and d_{yz} orbitals, which maintain the starting AO levels, are nonbonding MO's. However, in the present calculation, it can be seen that they have π interactions with p_x and p_y orbitals of the axially ligated atoms. As a results, it plays a role in reducing the energy difference between the $d_{z^2}(a_1'(\sigma^*))$ and d_{xz} (d_{yz}) $(e_1''(\pi^*))$ orbitals ($\Delta E_{xz}(\Delta E_{yz})$), so that the d–d transition may occur in the near-infrared region.

Discussion

Generally, an approximate linear relationship with a negative slope is expected between the g_z and A_z values for Cu(II) complexes with a $3d_{x^2-y^2}$ or $3d_{xy}$ ground-state,[26] because an A_z value can be expressed as Eq. 1 and $\Delta g_z \approx 4\Delta g_x$ (or Δg_y), which means that the latter can be neglected.[27] In the present study, a similar tendency could be seen for both the systems (Fig. 5a). However, compared with the case of a $3d_{x^2-y^2}$ or $3d_{xy}$ ground-state, these is very slight change in the g_z values, particularly for the BF_3–ether–water system, against the relatively large change in the A_z values. This can be explained as follows. In the case of a $3d_{z^2}$ ground-state, an A_z value is expressed as Eq. 2. Because of the reversal of the g anisotropy and $\Delta g_z \approx 0$ in this instance,[28] a correlation between the A_z and g_x (and/or g_y) values is expected. Actually, the obvious changes can be observed in the perpendicular components of the ESR spectra, as shown in Fig. 4, whereas the parallel components do not show any important change. An attempt has been made to show the relationship between the A_z and g_y values, as shown in Fig. 5b. The g_y values are preferred to the g_x values because the former are determined more exactly than the latter, and give a more remarkable change.

$$A_z = -P[\varkappa + \frac{4}{7} - \Delta g_z - \frac{3}{14}(\Delta g_x + \Delta g_y)] \quad (d_{x^2-y^2} \text{ or } d_{xy}), \quad (1)$$

$$A_z = -P[\varkappa - \frac{4}{7} - \Delta g_z + \frac{1}{14}(\Delta g_x + \Delta g_y)] \quad (d_{z^2}), \quad (2)$$

$$(\Delta g_z = g_z - g_e,\ \Delta g_x = g_x - g_e,\ \Delta g_y = g_y - g_e),$$

where P, $\varkappa$, and g_e have their usual meanings. Because of the positive sign of Δg_x and Δg_y, as shown in Eq. 2, there is a relationship with a positive slope. Of course, since Δg_x and Δg_y are divided by 14, it is natural that the A_z value is less dependent on the change in g values in the case of a $3d_{z^2}$ ground-state than in a $3d_{x^2-y^2}$ or $3d_{xy}$ one.

A Cu(II) complex with a $3d_{z^2}$ ground-state doublet is formed when an axial perturbation is stronger than an equatorial one in theory. However, there are few Cu(II) complexes with a $3d_{z^2}$ ground-state doublet because the more stable elongated conformation is easily formed, owing to the Jahn–Teller effect. On the other hand, 15C5 compounds easily produce unusual $3d_{z^2}$ ground-state Cu(II) complexes. One reason is that the cavity of the crown ether just fits the radius of the Cu(II) ion. Another important one is that the longer Cu–O distances in the equatorial positions are fixed by an ethylene group connecting the oxygen atoms. Consequently, the equatorial ligand field is weak, and an axial ligand can more close to the central atom without a larger repulsion from the equatorial atoms to provide a strong axial perturbation. It is thus certain that in forming a Cu(II) complex with a $3d_{z^2}$ ground-state doublet it may be a key point how to form a weaker equatorial ligand field as well as a stronger axial one. Thus, for the propose of understanding in more detail the coordination behavior of Cu(II) complexes with a $3d_{z^2}$ ground-state doublet, it is worth investigating the influence of the equatorial groups.

Considering the above-mentioned general relationships between the g and A_z values, one may have another question concerning how the substituents affect the g values. A qualitative answer is provided below. For a $3d_{z^2}$-type Cu(II) complex, the $g_{//}$ (g_z) and $g_\perp$ (g_x, g_y) values can be theoretically expressed as follows.[28] The shift in the $g_{//}$ values from g_e is ascribed to be a perturbation term of a second order, as shown in Eq. 3, since $g_{//}(=g_e)$ is a constant in a first-order condition:

$$g_{//} = g_e - 3\left(\frac{\alpha^2\lambda_0}{\Delta E_{xz,yz}}\right)^2, \quad (3)$$

$$g_\perp = g_e - \frac{6\alpha^2\lambda_0}{\Delta E_{xz,yz}}, \quad (4)$$

where $\Delta E_{xz,yz}$ corresponds to ΔE_{xz} (ΔE_{yz}), as previously defined. $\lambda_0(=-828\ \text{cm}^{-1})$ is the spin-orbit interaction parameter of a Cu(II)-free ion, and α^2 represents the spin density on the Cu(II) ion. In the present complexes, the stronger electron-withdrawing group tends to withdraw more electrons from the catechol oxygen atoms, and then from the Cu(II) ion, by an inductive effect through the benzene ring. That is

to say, the spin density on the Cu(II) ion (α^2) decreases (of course, it is also a reason that the A_z value becomes much smaller). Although the substituents have a slight influence on $\Delta E_{xy,yz}$, the stronger electron-withdrawing group causes a slight increase in $\Delta E_{xz,yz}$, because the d_{xz} and d_{yz} orbitals have a weak π interaction with the p_z orbitals of the catechol oxygen atoms. These facts are also supported by the EHMO calculation. Summarizing the above results, it is clear that the present Cu(II) complex with the stronger electron-withdrawing group will possess a smaller α^2 and a greater $\Delta E_{xz,yz}$. Thus, it is easy to understand, according to Eqs. 3 and 4, that the stronger electron-withdrawing substituent gives the larger $g_{//}$ and smaller $g_{\perp}$ values, while the electron-releasing one reverses those (note that λ_0 has a negative value).

Based on the EHMO calculations, one can judge the strength of a covalent bond from the atomic bond population. It is worth noticing that for all of the models the atomic bond populations of the axial Cu–O (or Cl) bonds are about three-times or more as large as those of the equatorial ones (for example, the axial atomic bond population calculated for **I** is 0.328 and the equatorial one is 0.111). Combining the MO calculation with the X-ray structure analyses, it can be said that the axial bonds are much stronger covalent bonds than the equatorial ones. Regarding the chemical bonding, Christe et al. proposed a model of IF_7, in which the five pentagonal ligands are bound in a semiionic bond, and the axial ligands are mainly covalently bonded through two sp_z hybrid orbitals of the central atom.[28] The present research supports the above conclusion. However, It is predicted that in the present complexes the axial ligands are bonded through two sd_{z^2} hybrid orbitals from the Cu(II) ion, as judged from the MO coefficients (Fig. 7).

As shown in Fig. 5, the Cu(II) complexes in the BF_3–ether–water system and in dry $CHCl_3$ have the same trend. However, the two systems exhibit a remarkable difference in the A_z values. Based on the X-ray and ESR results, the most important distinction concerning the structure for the two systems is the axial ligand, which is H_2O in the BF_3–ether–water system, and Cl^- in dry $CHCl_3$. H_2O is a stronger ligand than Cl^-. Neutral H_2O forms a more covalent bond with the Cu(II) ion, and pulls more charge from it; Cl^-, however, forms a weaker covalent bond, and its negative charge diminishes the force of further pulling charge from the Cu(II) ion. As a result, the spin density at the Cu(II) ion coordinated axially to water molecules has been guessed to be smaller than that of the chloride anions. This has in fact been demonstrated by a previous ESR study.[7b] It is thus natural that the present Cu(II) complexes in the BF_3–ether–water system have smaller A_z values. In contrast with the case of dry $CHCl_3$, the changes in the A_z and g values, caused by substituent effects, is relatively small in the BF_3–ether–water system. One of the reasons is presumed that, as mentioned above, the spin density at the Cu(II) ion is lower in the BF_3–ether–water system than in dry $CHCl_3$; thus, the change in the spin density due to the substituent effect is also comparatively small, and, consequently, smaller changes in the g and A_z values are observed in the BF_3–ether–water system. Another one is considered to be that the Cu(II) complexes with axial coordinated water molecules have a more compact coordination geometry, as derived from the abovementioned X-ray structure analyses. Therefore, the conformation of the crown ether, which may be influenced by a change in the charge population, is slightly more affected by the substituents.

The author would like to express his sincere thanks to Professor Jun Yamauchi of Kyoto University for his encouragement and useful discussions. He is particularly indebted to Professor emeritus Kazuhiko Ishizu, Professor Nagao Azuma and Dr. Kunihiko Tajima (now moved to Kyoto Institute of Technology) of Ehime University for the X-ray measurements and helpful discussions and continuous concern about this work.

References

1) A. Abragam and B. Bleaney, "Electron Paramagnetic Resonance of Transition Ions," Clarendon Press, Oxford (1970).

2) a) J. D. Swalen, B. Johnson, and H. M. Gladney, *J. Chem. Phys.*, **52**, 4078 (1970); b) K. T. McGregor and W. E. Hatfield, *J. Chem. Soc., Dalton Trans.*, **1974**, 2448; c) R. Hirasawa and H. Kon, *J. Chem. Phys.*, **56**, 4467 (1972).

3) a) R. Barbucci, A. Bencini, and D. Gatteschi, *Inorg. Chem.*, **16**, 2117 (1977); b) D. Reinen and C. Friebel, *Inorg. Chem.*, **23**, 791 (1984).

4) a) K. Ishizu, T. Haruta, K. Miyoshi, and Y. Sugiura, *Chem. Lett.*, **1978**, 579; b) K. Ishizu, T. Haruta, Y. Kohno, K. Mukai, and Y. Sugiura, *Bull. Chem. Soc. Jpn.*, **53**, 3513 (1980).

5) K. A. Klanderman, W. C. Hamilton, and I. Bernal, *Inorg. Chem. Acta*, **23**, 117 (1977).

6) T. Sakurai, K. Kobayashi, S. Tsuboyama, Y. Kohno, N. Azuma, and K. Ishizu, *Acta Crystallogr., Sect. C*, **39C**, 206 (1983).

7) a) Y. Li, H. Tomoda, K. Tajima, K. Ishizu, and N. Azuma, *Chem. Lett.*, **1985**, 961; b) Y. Li, K. Tajima, K. Ishizu, and N. Azuma, *Bull. Chem. Soc. Jpn.*, **60**, 557 (1987).

8) a) C. J. Pedersen, *J. Am. Chem. Soc.*, **98**, 7017 (1967); b) U. Takaki, T. E. Hogen Esch, and J. Smid, *J. Am. Chem. Soc.*, **93**, 6760 (1970); c) M. Bourgoin, K. W. Wong, J. Y. Hui, and J. Smid, *J. Am. Chem. Soc.*, **97**, 3462 (1975); d) R. Ungano, B. El Haj, and J. Smid, *J. Am. Chem. Soc.*, **98**, 5198 (1976); e) S. S. Moore, T. L. Tarnowski, M. Newcomb, and D. J. Gram, *J. Am. Chem. Soc.*, **99**, 6398 (1977).

9) In a BF_3–ether–water system, B15C5 can form a $3d_{z^2}$-type Cu(II) complex in an equivalent metal/ligand molar ratio, as previously reported.[7b] However, a decreasing in complexation ability for 4′-substituted B15C5 was found in the present work, taking account of the fact that components due to $3d_{x^2-y^2}$ or $3d_{xy}$-type Cu(II) complexes were observed in ESR spectra when the Cu(II)/ligand molar ratio was larger than about 1/1.1. On the other hand, it is interesting that $3d_{x^2-y^2}$ or $3d_{xy}$-type components are also detected for 4′-substituted B15C5 containing a carbonyl group, if the Cu(II)/ligand molar ratio is too small. It may be explained that a Cu(II) ion is coordinated to several carbonyl groups of the crown ether molecules when the amount of the crown ether is much more than that of the Cu(II) ion.

10) A. C. T. North, D. C. Phillips, and F. S. Mathews, *Acta Crystallogr., Sect. A*, **24A**, 351 (1968).

11) a) C. J. Gimore, *J. Appl. Cryst.*, **17**, 42 (1984); b) J. C.

Calbrese, Ph. D. Thesis, University of Wisconsin-Madison, (1972); c) P. T. Beurskens, *Technical Report 1984/1*, Crystallography Laboratory, Toernooiveld, 6525Ed, Nijmegen, Netherlands.

12) "TEXSAN—Texray Structure Analysis Package, Version 5.0," Molecular Structure Corporation, The Woodlands, TX77381 (1989).

13) "International Tables for X-Ray Crystallography," Kynoch Press, Birmingham (1974), Vol. IV.

14) K. Nishimoto, A. Imamura, K. Yamaguchi, S. Yamabe, and K. Kitaura, "Bunshisekkei notameno ryoushikagaku," Koudansha, Tokyo (1989).

15) EHMO calculations were also carried out for $[Cu(15C5)(H_2O)_2]^{2+}$, $[Cu(B15C5)(H_2O)_2]^{2+}$, and $[Cu(B15C5)Cl_2]$ by using the geometries obtained from the X-ray analyses. Because of reduction in symmetry, the calculated results become more complicated. However, one can find the corresponding relationship to the results of the models discussed in detail, and obtain the similar conclusions.

16) R. C. Weast and M. J. Astle, "CRC Handbook of Chemistry and Physics," 62nd ed, CRC Press Inc., Florida (1981).

17) C. J. Ballhausen and H. B. Gray, "Molecular Orbital Theory," Benjamin Inc., New York (1964).

18) R. H. Sumnerrille and R. Hoffmann, *J. Am. Chem. Soc.*, **98**, 7240 (1975).

19) J. W. Richardson, W. C. Nieuwpoort, R. R. Powell, and W. F. Edgell, *J. Chem. Phys.*, **36**, 1057 (1962).

20) J. H. Ammeter, H.-B. Burgi, J. C. Thibeault, and R. Hoffmann, *J. Am. Chem. Soc.*, **100**, 3686 (1978).

21) S. Motherwell and W. Clegg, "PLUTO-Program for Plotting Molecular and Crystal Structures," University of Cambridge, U. K. (1978).

22) R. D. Shannon, *Acta Crystallogr., Sect. A*, **32A**, 751 (1976).

23) J. Gazo, I. B. Bersuker, J. Garaj, M. Kabesova, J. Kohout, H. Langfelderova, M. Melnik, M. Serator, and F. Valach, *Coord. Chem. Rev.*, **19**, 253 (1976).

24) R. Hoffmann, *J. Chem. Phys.*, **39**, 1397 (1963).

25) a) J. J. Zucherman, *J. Chem. Educ.*, **42**, 315 (1965); b) R. Krishnamurthy and W. B. Schaap, *J. Chem. Educ.*, **46**, 799 (1969).

26) J. Peisach and W. G. Blumberg, *Arch. Biochem. Biophys.*, **165**, 691 (1974).

27) J. R. Pilbrow, "Tansition Ion Electron Paramagnetic Resonance," Clarendon Press, Oxford (1990).

28) K. O. Christe, E. C. Curtis, and D. A. Dixon, *J. Am. Chem. Soc.*, **115**, 1520 (1993).